EEET ECOLOGICAL ENGINEERING & ENVIRONMENTAL TECHNOLOGY

Ecological Engineering & Environmental Technology, 2025, 26(8), 329–341
https://doi.org/10.12912/27197050/207282
ISSN 2719–7050, License CC-BY 4.0

Received: 2025.05.26
Accepted: 2025.07.18
Published: 2025.08.01

Predicting land use land cover dynamics using machine learning and satellite imagery: A case study

Brahim Meskour[1*], Mohammed Hssaisoune[1,2,3], Adnane Labbaci[1], Zouhir Dichane[4], Mohamed Aghenda[1], Yohann Cousquer[5], Lhoussaine Bouchaou[1,3]

[1] Applied Geology and Geo-Environment Laboratory, Faculty of Sciences, Ibn Zohr University, Agadir, 80035, Morocco
[2] Faculty of Applied Sciences, Ibn Zohr University, B.O. 6146 Azrou District, 86153, Ait Melloul, Morocco
[3] Mohammed VI Polytechnic University, International Water Research Institute, Ben Guerir, 43150, Morocco
[4] Geoengineering and Environment Laboratory, Research Group "Water Sciences and Environment Engineering", Geology Department, Faculty of Sciences, Moulay Ismail University, Zitoune, Meknes BP 11201, Morocco
[5] HSM, Univ. Montpellier, CNRS, IMT, IRD, Montpellier, France
* Corresponding author's e-mail: brahim.meskour@edu.uiz.ac.ma

ABSTRACT

Land use and land cover (LULC) change is an important factor when solving environmental issues, such as water resources, agricultural productivity, and soil preservation. This study looked at the spatial and temporal trends of LULC over a 33-year period, in an area of the Sebou basin in Morocco, while forecasting future patterns, and investigating predictive performance from several machine learning classification models. A supervised classification was applied using satellite imagery from 1993, 2003, 2013, and 2023. The three different classification methods used the gradient boosting machine (GBM), support vector machine (SVM), and random forest (RF) to classify the land use and land cover into four major LULC categories: vegetation/forest, built area, bare land, and water. In predicting the land use and land cover class for 2033, a Cellular Automata – Artificial Neural Network (CA-ANN) was applied in QGIS using the MOLUSCE plugin. The GBM model was more accurate than the others with Kappa coefficients of 95.9 in 1993, 93.3 in 2003, 94.4 in 2013, and 99.8 in 2023. The overall Kappa index for the validation of the 2023 classification was 77%. Results indicate that bare land and built-up areas are on the rise as a consequence of anthropogenic activities, at the expense of vegetation and forest cover. Such changes present a source of concern for long-term sustainability, and resource availability. The study accuracy depends on the quality and resolution of the satellite data used, while assumptions in the simulation models can also introduce uncertainty in future projection. The findings of this analysis provide critical information that will support and help implement and informed policy and planning in the area of sustainable land management and protection. The research incorporated various methodological approaches in one study, thus combining LULC analyses into one study, and performing comparative analyses utilizing machine learning methods, as well as predictive modeling studies in an applied context to carry out monitoring and forecasting land use dynamics in susceptible areas.

Keywords: supervised classification, machine learning, degradation land, MOLUSCE.

INTRODUCTION

Worldwide, the agroforestry systems are facing an increase in degradation, threatening the survival of species vital for food supply. Vegetation is a crucial component and an integral part of the soil-vegetation-atmosphere nexus, However, the climate change global impact has caused shifts in land ecosystems (Luo et al., 2020). These dynamics are driven by both natural processes and human activities. In agroecosystems, crop yield productivity is controlled by human-environment interactions. This parameter is essential for the maintenance of contemporary human societies

(Martin et al., 2019). Furthermore, mitigation and adaptation when implemented together, and combined with broader sustainable development objectives, would yield multiple benefits for human well-being as well as ecosystem and planetary health (IPCC (2013)., n.d.).

Land degradation stands out as a crucial and important challenge in contemporary times (Elaloui et al., 2022; Labbaci and Bouchaou, 2022). The effect of climate change and population growth, along with factors such as deforestation, floods, Health of vegetation, and droughts, are among the key contributors to land degradation (Ouassanouan et al., 2022; Saddik et al., 2024). One of the most critical problems in agroforestry is LULC change. However, monitoring and mitigating the effects of LULC changes is crucial for various purposes that impact human welfare, particularly in the context of rapid, uncontrolled population growth, ongoing economic and industrial development (Talukdar et al., 2020). Therefore, it is an essential input for a variety of scientific studies, such as urban and regional planning (Idoumskine et al., 2024), environmental vulnerability and impact assessment (Fei et al., 2018), natural disasters and hazard monitoring (Hadri et al., 2021), groundwater management (Ait Brahim et al., 2017) as well as estimation of soil erosion and salinity (Borrelli et al., 2020). This need is especially pressing in developing countries, where intensified LULC changes are more prevalent. These changes exert a range of effects on human society and agroforestry, including heightened vulnerability to drought, environmental degradation, depletion of groundwater resources, increased risk of landslides, and soil erosion (Agidew and Singh, 2017; Akinyemi, 2021; Loukika et al., 2021).

Various research efforts aimed to adapt and mitigate the impacts of climate change on agricultural practices and groundwater resources in semi-arid countries, such as Morocco (Bouchaou et al., 2011; Ongoma et al., 2024; Ouazar et al., 2017). Additionally, it can support researchers as they look into diverse environmental challenges at different scales. However, LULC maps can be helpful in identifying the areas influenced and affecting the water resources and land, which are valuable for general watershed management.

Recently, satellite imagery processing such as Landsat and Sentinel was used as free open access. These images increased the use of machine learning images as classifiers for remote sensing. This plays an important role in producing LULC maps (El Hachimi et al., 2022; Idoumskine et al., 2024). In addition, it has been popularly used for the monitoring of environmental phenomena, including ecosystem assessment (Tavares et al., 2019) identifying agricultural systems, and crop mapping (Htitiou et al., 2019), as well as assessing desertification, drought, and water erosion (Ayugi et al., 2020; Hakam et al., 2024; Labbaci and Bouchaou, 2022). This technique can help to find a solution to address the ecosystem degradation effect.

Machine learning (ML) and deep learning algorithms are predominantly utilized in supervised classification. Various algorithms employed for LULC mapping include gradient boosting machines, artificial neural networks (ANN), RF, support vector machines (SVM), decision trees (DT), k-nearest neighbors (KNN), and maximum likelihood estimation (Akinyemi, 2021; Azimi Sardari et al., 2019; Esmail et al., 2016; Muto et al., 2022).

Research in Mediterranean countries, such as Morocco, is used for mapping the agriculture and forest land to monitor and assess the agricultural land change (El Haj et al., 2023; Mohajane et al., 2018). The LULC changes driven by a rapidly increasing population represent a significant challenge for developing nations, such as Morocco, particularly in urban regions. The degree, intensity, location, and type of human-induced modifications to the natural land cover within a watershed determine the impact of LULC on that catchment. This research utilized Landsat satellite data as well as three machine learning classifiers (SVM, RF, and gradient boosting (GB)) to undertake a multi-temporal analysis of LULC dynamics over a 30 year period (1993–2023). The purpose of this study was to examine the efficiency of the algorithm and its ability to classify LULC data consistently and correctly over time. The MOLUSCE tool then takes the best model for classifying LULC and estimates future trajectories of LULC dynamics. This study provides a best practice approach and fills a substantial information void in the current literature by providing an exhaustive comparison of ML classifiers used to monitor long-term LULC in a semi-arid watershed in order to enhance potential predicted accuracy in land change modeling. This study is expected to identify ensemble methods such as GB and RF that will have better temporal stability (robust) and overall accuracy than SVM.

MATERIAL AND METHODS

Study area

The Oued Ouergha watershed serves as the case study and is located within the Sebou Hydraulic Basin Agency's (ABHS) action area. The Rif to the north, the Middle Atlas and Meseta to the south, the Fes-Taza region to the east, and the Atlantic Ocean to the west all converge to form the Sebou basin (Figure 1).

The study area takes place in the Sebou basin. It is the watershed of the Koudiat Borna Dam (BKB) site. The one on the Ouergha river has a perimeter of 167.40 km and covers an area of approximately 1021 km², which represents 1.14% of the Oued Sebou watershed of which it is part. The basin located in its downstream part on the north side of the basin is bounded to the west by the Oued Rdat basin, to the east and south by the Oued Sebou basin, and to the north by the Loukouss basin. The dam site is located on the Oued Ouergha in the province of Sidi Kacem, about 30 km north of the city of Sidi Kacem, and about 9 km northeast of the village of Khenichet.

The watershed is subject to a semi-continental climate, characterized by a temperate and humid winter and a hot and dry summer. This situation means that the rainy year consists of two contrasting seasons, a wet season that extends from October to May, and another dry one from June to September.

Data

The dataset used in this study mostly consisted of field data and satellite images. Specifically, the images from the Landsat 5 Multispectral Scanner (MSS), Landsat 7 Enhanced Thematic Mapper Plus (ETM+), and Landsat 8 Operational Land Imager (OLI) pertaining to the Koudiat Borna dam basin were sourced from https://earthexplorer.usgs.gov/ for the years 1993, 2003, 2013, and 2023, adhering to a maximum cloud cover threshold of 10%. These images were subsequently uploaded and preprocessed using the Google Earth Engine platform (https://earthengine.google.com).

Methodology

Figure 2 shows the methodology adopted in this study for monitoring changes in LULC. First, the Landsat Collection 2, Level 2 (C2 L2) imagery was preprocessed in the GEE platform, where radiometric and atmospheric corrections were applied. Secondly, the training and testing samples that served as reference data were carefully designed to reflect five LULC classes: Build up, Bare soils, Agriculture, Forest and water. Third, multiple classifiers were used to classify the image of the research area between 1993 and 2023. Finally, the kappa indices (KI) and overall accuracy (OA) were used to assess the outcomes of various categorization techniques.

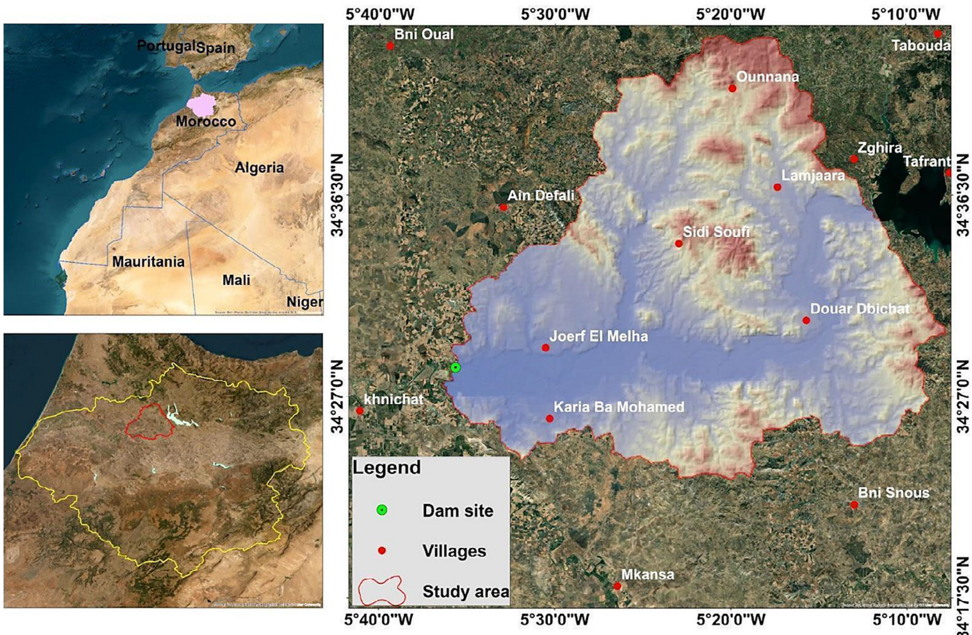

Figure 1. Geographic location of study area

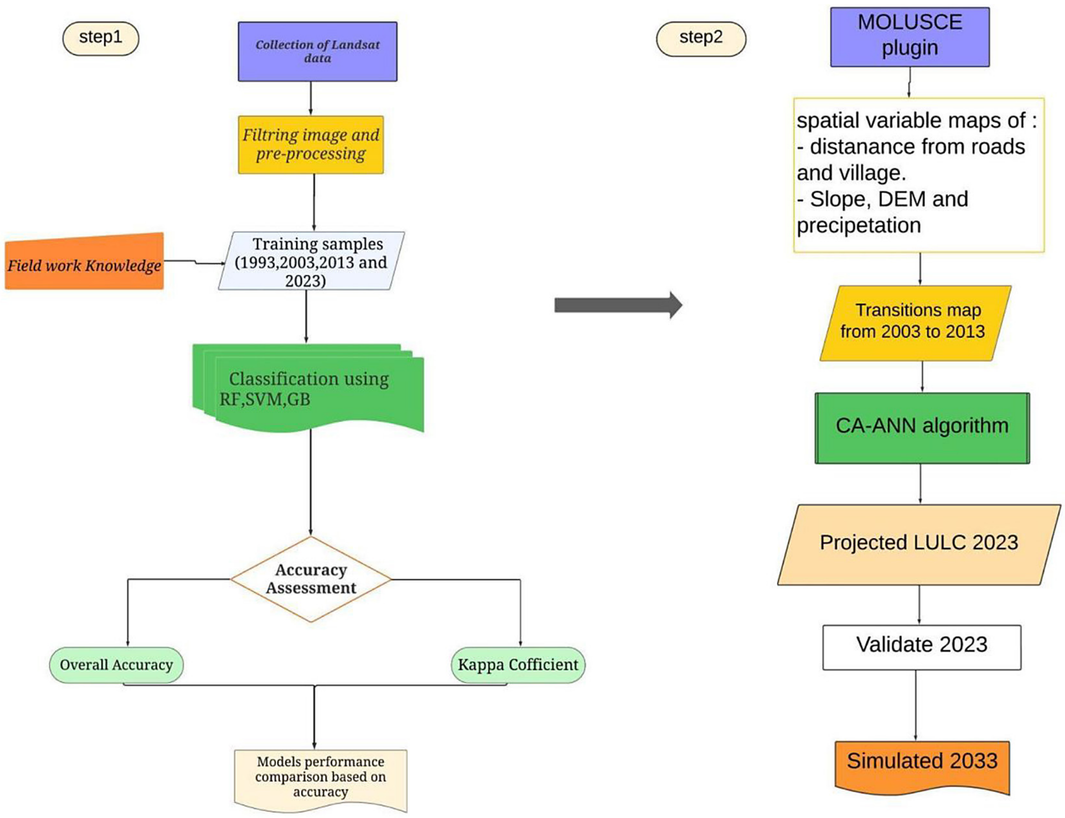

Figure 2. Methodology for classifying actual and future forecast LULC maps on GEE

In order to enhance the quality of the satellite images, the Landsat satellites 5, 7, and 8 undergo necessary preprocessing operations before delivering high-resolution (30 m) observations of the Earth's surface. The median was used to aggregate Landsat data for the full year. Normalized difference vegetation index (NDVI), Normalized difference water index (NDWI), Bare soil index (BSI) and normalized difference build index (NDBI) are four spectral indices used for the categorization of LULC. They are reflective of vegetation features and water bodies, respectively. The land cover types seen in the Landsat data are categorized using the characteristics that were extracted. For classification, three machine learning algorithms RF, SVM and GB are used. Accurate land cover maps are validated and the classifier is trained using training samples as well as ground truth data. The accuracy of the classification is determined through a comparison between the classified outcomes and real-world data or established datasets. Metrics like overall accuracy and kappa indices are computed to evaluate the performance of the classification algorithm. Analyzing the generated LC maps can yield important information on vegetation behavior, urbanization, environmental changes, and other relevant applications.

Calculation of indices

The Landsat surface reflectance bands, including Blue (B2), Green (B3), Red (B4), Red Edge 1

Table 1. Formulas of the used vegetation indices

Acronym	Designation	Equation	References
NDWI	Normalized difference water index	$\frac{G - NIR}{G + NIR}$	(McFeeters, 1996)
NDBI	Normalized difference built up index	$\frac{SWIR1 - NIR}{SWIR1 + NIR}$	(Zha et al., 2003)
NDVI	Normalized difference vegetation index	$\frac{NIR - RED}{NIR + RED}$	(Rouse et al., 1974)
BSI	Bare soil index	$\frac{(SWIR1 + RED) - (NIR + BLEU)}{(SWIR1 + RED) + (NIR + BLEU)}$	(Rikimaru et al., 2002)

(B5), Red Edge 2 (B6), Red Edge 3 (B7), Near Infrared (NIR, B8), Shortwave Infrared 1 (SWIR 1, B11), were utilized to establish the initial feature set for land cover classification. Additionally, four indices were integrated into the training dataset to ensure precise classification (Table 1). Remote sensing provides a plethora of indices suitable for LULC classification tasks, among which the NDVI is a commonly used indicator.

Classification algorithms

- Support vector machine

SVMs are a set of algorithms that specialize in resolving regression and mathematical discrimination issues through the use of supervised learning. They were created by Vladimir Vapnik in 1998 (Vapnik 1998). SVM has the ability to address two distinct scenarios: in the cases where classes can be separated by a straight line, the algorithm aims to find a linear decision boundary known as a hyperplane. This hyperplane is designed to minimize generalization error while maximizing the margin between the two classes (Pal and Mather 2005).

- Random forest

Random forest (RF) is an ensemble-based supervised classification strategy that combines bagging and the random subspace method (Breiman 2001). The method creates many decision trees to generate class output. There is no need to make assumptions about the input or output variables. The key advantage of this method is its ability to handle diverse data sets, including satellite data (Breiman, 2001). The efficacy of the RF algorithm is assessed by employing non-training samples, ensuring a fair validation process separate from the training data. This validation approach guarantees a robust evaluation at each node, facilitating the creation of a valid separation between classes (Zhao et al. 2024).

Gradient boosting

Similar to RFs, gradient boosting decision trees (GBDT), as introduced by Friedman in 2001, indicate an ensemble model based on decision trees. Two important differences exist between GBDT and RF, though. While RFs use a bagging technique to build individual trees individually in order to improve accuracy through variance reduction, GBDTs first construct an ensemble in a sequential manner with the aim of increasing accuracy through bias reduction.

Extreme gradient boosting (Xgboost) is currently a highly preferred GBM approach, especially in the remote sensing industry (Jun 2021). The distinctive advantage of Xgboost over other algorithms lies in its approach to constructing an objective function. This function not only encompasses the loss function, which measures prediction accuracy, but also integrates a regularization component. This regularization term is crucial for managing the model's complexity, helping to prevent overfitting by penalizing more complex models.

Accuracy assessment

Accuracy evaluation in categorization is crucial for determining the best sustainable land management approach (Deng et al., 2008). The training input were separated into training and validation sets. LULC mapping frequently employs accuracy evaluation metrics such as overall accuracy (Equation 1) and kappa coefficient (Equation 2) on complete training datasets (El Hafyani et al., 2021). Each class's accuracy was determined using the LULC classes' tabulated square confusion matrix.

$$Overall\ accuracy\ OA = 100\ \frac{\sum_{i=1}^{m} Pii}{n} \tag{1}$$

$$The\ kappa\ coefficient\ K = \\ = \frac{\sum_{i=1}^{m} Pii - \sum_{i=1}^{c} Pi + P + i}{n^2 - \sum_{i=1}^{m} Pi + P + i} \tag{2}$$

Prediction of LULC

Future LULC modifications were analyzed and modeled using QGIS's MOLUSCE Plugin 4.0.0. This tool helps assess the overall change in land cover, simulate dynamic changes, and validate the model's results (Muhammad et al., 2022). The analysis covered the LULC transitions from 2003 to 2013, generating a transition matrix and change probability matrix. Variables such as DEM data, distance to villages, slope, precipitation, and proximity to roads were considered, as these factors influence LULC variation.

For the 2023 forecast, the CA-ANN algorithm within MOLUSCE was applied to model transformation potential and create a simulated LULC map based on the changes observed between 2003 and 2013. The simulated 2023 map was then compared with the actual 2023 LULC map to assess accuracy, using the Kappa coefficient for validation (Phuong et al., 2023).

Next, the simulation of LULC changes for 2033 was performed using the data from the 2013–2023 period. This helped in predicting how land cover might evolve over the following decade.

Lastly, the rate of change for each LULC type was calculated using formula (3):

$$\Delta\,(\%) = (Fy - Iy)\,/\,S \times 100 \quad (3)$$

where: Δ represents the rate of area change, *Fy* and *Iy* are the land cover areas at the beginning and end of the period, and *S* is the total area of the study.

RESULTS

LULC classification

This study assessed the performance of three machine learning approaches, GB, SVM, and RF, for LULC categorization of study areas. The LULC maps produced are shown in Figure 3. The classification results reveal five distinct classes: bare land, forest, buildup, agriculture, and water. Across all three algorithms employed, the surface area of bare land and buildup has shown an increase over the years, while agriculture and forest cover have demonstrated a decrease from 1993 to 2023 (Figure 4).

Classification performances

The evaluation of accuracy was carried out to assess the effectiveness of various algorithms. The metrics most frequently employed for this evaluation are OA and KC, which indicate the percentage of correctly classified test data and the level of agreement between predicted and actual classifications beyond mere chance, respectively.

Training and validation were performed utilizing the GB classifier for the years 1993, 2003, 2013, and 2023. The findings indicated that the GB classifier consistently achieved high performance in terms of overall accuracy (OA) and Kappa coefficient (KC) across these years. Notably, in 2023, the GB classifier reached an OA of 0.99 and a KC of 0.99. In 2013, it recorded an OA of 0.94 and a KC of 0.94, while

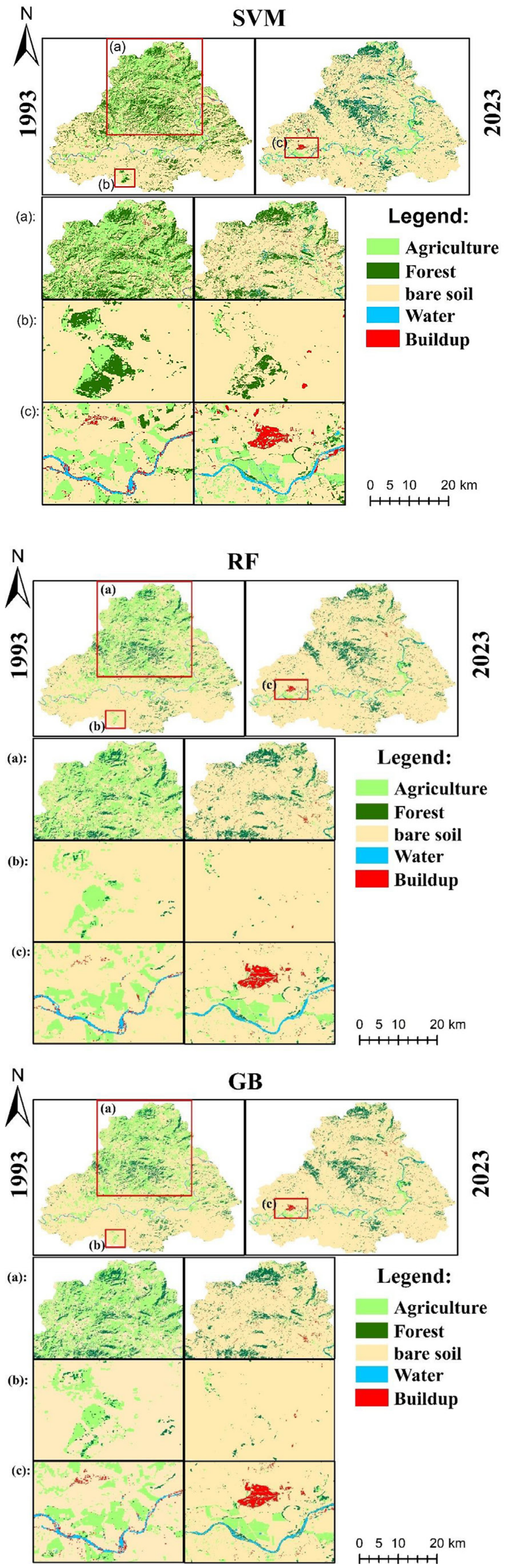

Figure 3. LULC maps of Landsat images using SVM, RF, and GB classifiers for the years 1993, 2003, 2013, and 2023

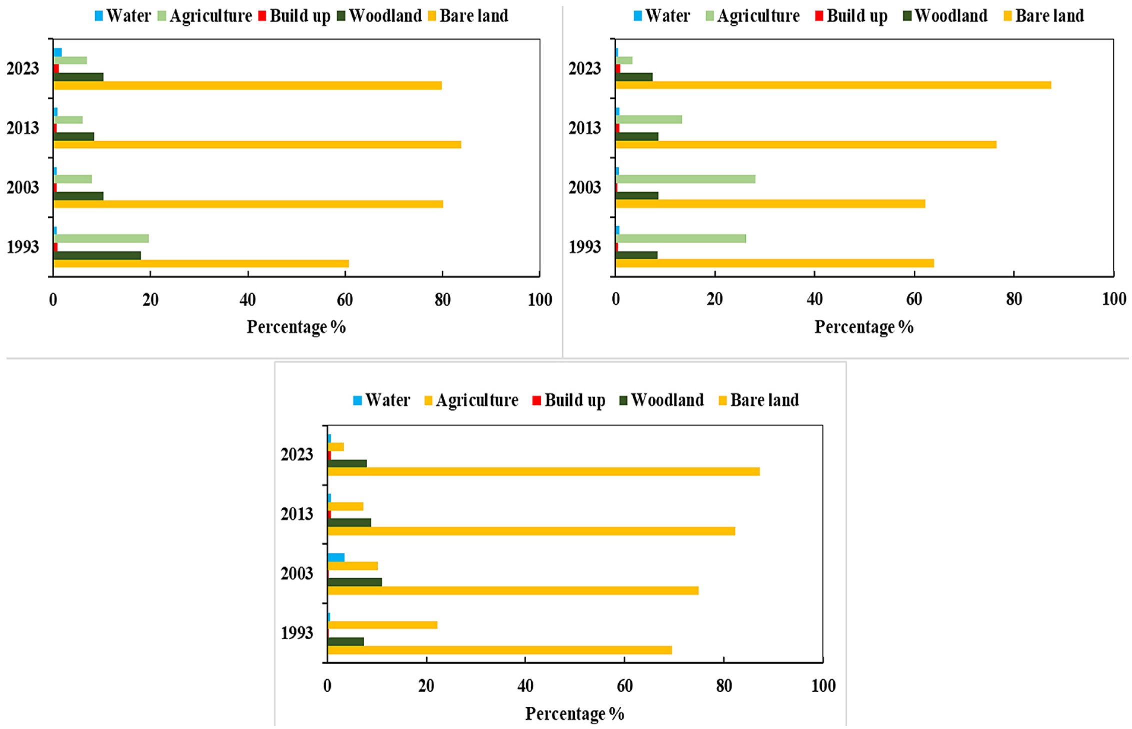

Figure 4. LULC change for RF, SVM, and GB models

in 1993, it documented an OA of 0.91 and a KC of 0.91 (Table 2).

These findings underscore the superior performance of the GB classifier relative to SVM and RF regarding both accuracy and reliability across varying time periods.

LULC prediction

The analysis integrated the historical changes in LULC with spatial variables, specifically digital elevation model (DEM) data and proximity to roads (Figure 5). The cellular automata-artificial neural network (CA-ANN) algorithm, implemented within the MOLUSCE plugin, was employed to conduct simulations of LULC for the year 2033. Initially, the data on LULC changes from the period 2003 to 2013 served as a foundation for constructing a simulated LULC map for 2023 (simulated 2023). This simulated map was subsequently compared to the actual LULC map for 2023 and validated with an overall Kappa

Table 2. Kappa coefficient and overall accuracy for different machine learning classifiers

Year	Classifiers	Landsat images	
		Overall accuracy (%)	Kappa coefficient
1993	SVM	0.802	0.692
	RF	0.936	0.907
	GB	0.959	0.941
2003	SVM	0.758	0.627
	RF	0.922	0.880
	GB	0.933	0.898
2013	SVM	0.908	0.861
	RF	0.938	0.908
	GB	0.944	0.916
2023	SVM	0.929	0.988
	RF	0.956	0.978
	GB	0.998	0.998

index of 77%. This step helps to ascertain the accuracy of the projected LULC map for 2033 (predicted 2033) (Figure 6).

LULC transition analysis

During the decade spanning from 2003 to 2013, 12% of the agricultural area remained unchanged. Additionally, there was a reduction in this area by 15%. This decline can be attributed to conversions to bare soil (80%), forest (7%), built-up areas, and water bodies (0.5%). Specifically, the forested area experienced a decrease of 0.12%, primarily due to a reduction in density over the ten-year period. Conversely, the buildup area exhibited significant variation, increasing from 0.34% to 0.85%. Furthermore, the amount of bare soil increased from 2003 to 2013, while water area in streams remained stable throughout this timeframe (Figure 7).

Table 3 reveals major shifts in land usage across the three periods (2003–2013, 2013–2023, 2023–2033). From 2003 to 2013, agricultural land shrank by 14,819 ha (-14.65%), while bare ground grew by 14,339 ha (+14.18%) hinting at farmers leaving their fields or changing land use. Forests saw a small drop (-159 ha, -0.16%), as cities expanded a bit (+507 ha, +0.5%). Water class has slightly increased by 133 ha (+0.13%).

In 2013-2023, this pattern kept up with farmland losing more ground (-9,966 ha, -9.85%) and bare soil gaining even more (+11,152 ha, +11.02%). Forests keep shrinking (-1,052 ha, -1.04%), while cities grow a tiny bit (+62 ha +0.06%). Unlike before, water areas shrunk by 196 ha (-0.19%).

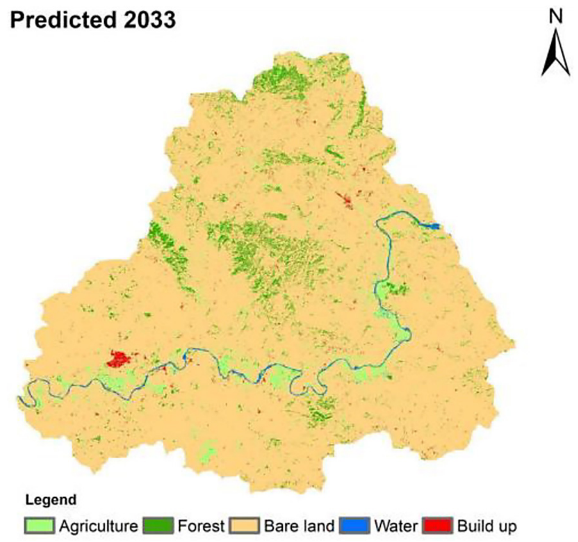

Figure 6. LULC Map predicted

For 2023–2033, farmland bounced back a little (+944 ha +0.92%), but forests lost ground faster (-2,229 ha, -2.18%). Bare soil kept growing (+1,381 ha, +1.35%), and water areas stayed about the same (-2 ha, -0.002%). Cities shrunk by 95 ha (-0.09%), which might mean city growth is slowing down.

These results indicate continued pressure on agricultural and forest land in favor of bare soil and built-up areas, with potential impacts on biodiversity and water resources.

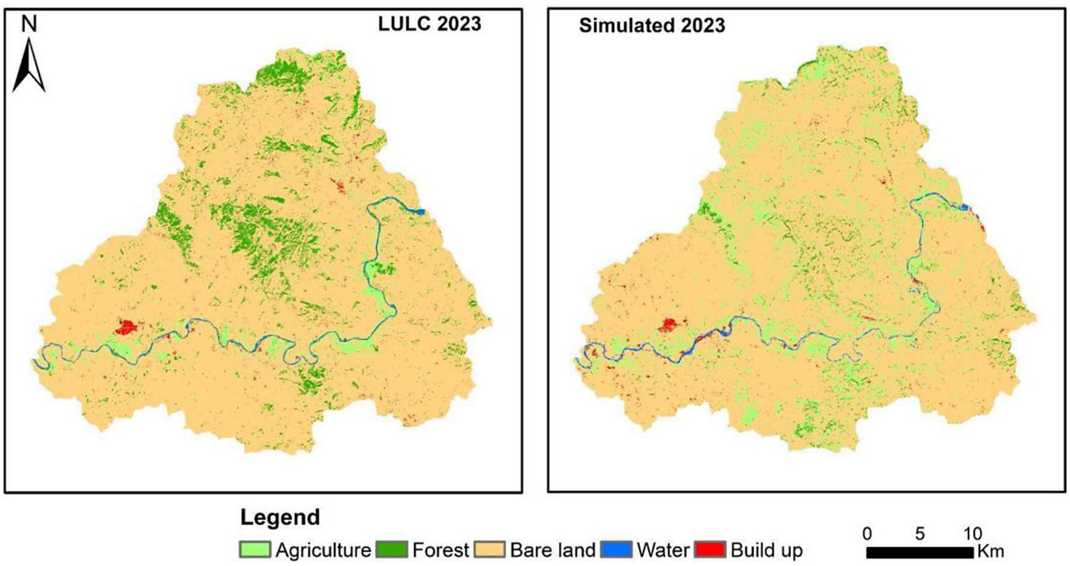

Figure 5. LULC maps generated and simulated

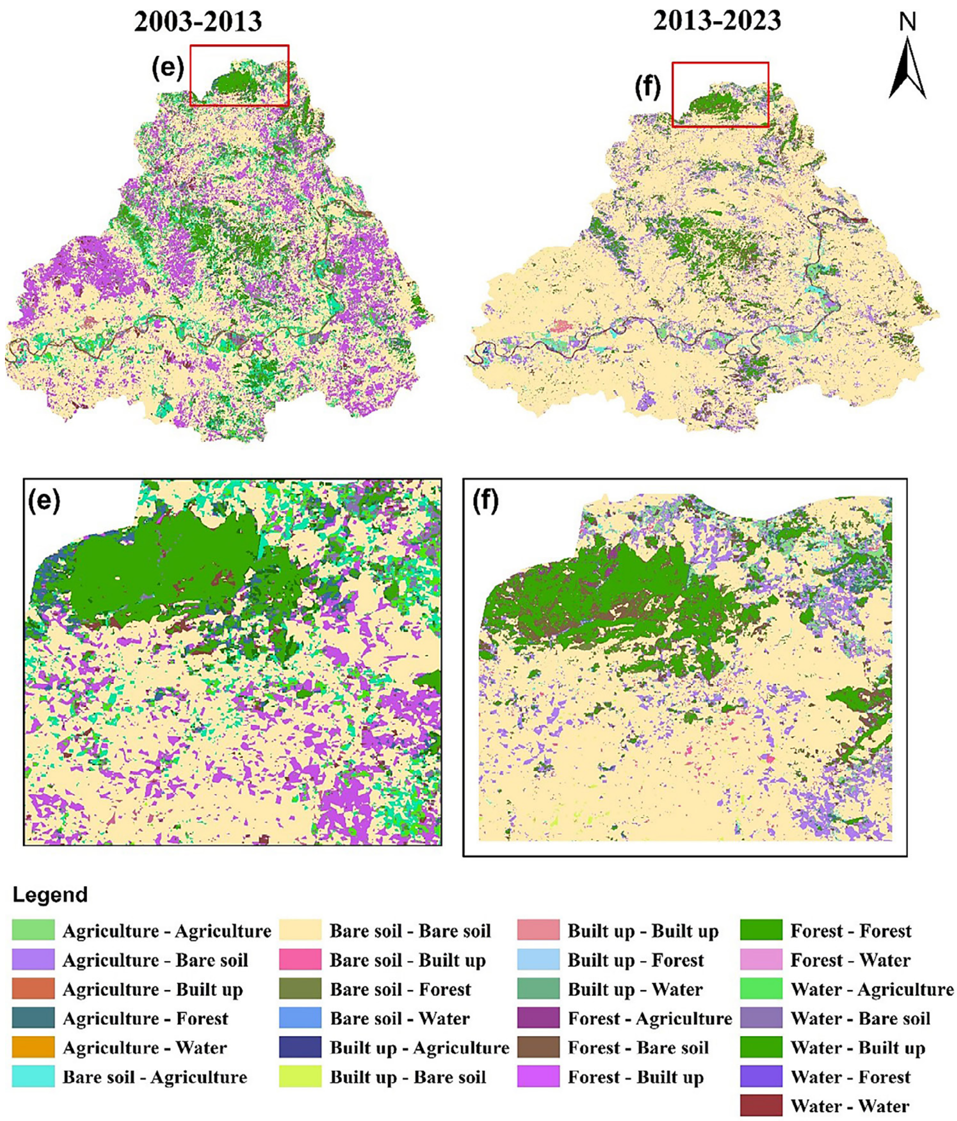

Figure 7. LULC transition matrix for periods 2003–2013 and 2013–2023

DISCUSSION

Comparison of accuracy of three algorithms

Previous research has shown that the distribution of LULC classes exhibits considerable variation depending on the classification methods employed, whether they be machine-learning algorithms or traditional techniques. In this study, the authors aimed to identify the dynamics of LULC over the 33 years and predict the changes by 2033 in KB basin dam. However, the comparative study of the machine learning algorithms (GB, RF, and SVM) was aimed at determining the most accurate and most reliable algorithm to classify LULC changes over time and gain a better understanding of land transformation processes. The aim of forecasting future LULC using the CA-ANN model was to simulate land use scenarios and gauge forthcoming environmental and planning issues. In this analysis, satellite imagery, ground truth data, and index data with three machine learning algorithms were used. The model that demonstrated superior performance, as determined by accuracy and kappa coefficient metrics, was subsequently utilized for predictive modeling. In addition to improving the knowledge of land cover dynamics, this method makes it easier to predict future changes in land cover.

Figure 3 shows clear land cover changes from 1993 to 2023 using SVM, RF, and GB models. There is a steady decrease in forest cover and an increase in farmland and bare soil, particularly in the watershed's center and southern regions. Zones of notable land alteration and environmental stress are revealed by these patterns. For the

Table 3. Multi-temporal LULC transition area

Parameter	2003	2013	Δ (ha)	2003%	2013%	Δ %
Agriculture	28310.31	1349.91	-14819.40	27.992	13.339	-14.65
Forest	8807.40	8648.37	-159.03	8.708	8.551	-0.157
Baresoil	62999.46	77338.80	14339.34	62.29	76.47	14.178
Water	671.94	804.51	132.57	0.664	0.795	0.131
Build up	345.24	851.76	506.52	0.341	0.842	0.5008
	2013(Ha)	2023(ha)	Δ (ha)	2013%	2023%	Δ %
Agriculture	13504.14	3538.26	-9965.88	13.34	3.495	-9.846
Forest	8662.23	7609.86	-1052.37	8.558	7.518	-1.039
Baresoil	77387.58	88539.48	11151.90	76.46	87.48	11.018
Water	805.05	609.39	-195.66	0.795	0.6020	-0.193
Build up	852.21	914.22	62.01	0.8420	0.9023	0.06
	2023	2033	Δ (ha)	2023%	2033%	Δ %
Agriculture	3544.02	4488.26	944.26	3.4720	4.39	0.92
Forest	7631.08	5402.50	-2228.58	7.4760	5.29	-2.18
Baresoil	89367.16	90748.44	1381.27	87.552	88.90	1.353
Water	608.97	606.63	-2.34	0.5966	0.594	-0.002
Build up	921.87	827.25	-94.62	0.90	0.810	-0.092

first time, this study pinpoints specific areas of land degradation and forest loss, providing important information for planning resilience and future land management. As illustrated in Figure 4, the GB model plays a significant role in evaluating the accuracy of classification outcomes. In similar contexts, prior research has employed remote sensing classification methodologies (Zhao et al. 2024). The comprehensive results of the present study underscore the superior efficacy of the Random Forest (RF) technique when compared to SVM (McCarty, Kim, and Lee 2020). With respect to overall accuracy, the classification findings reveal that LightGBM attained the highest OA of 0.653, closely followed by SVM with an OA of 0.642, and subsequently RF with an OA of 0.594. (Ouzemou et al., 2018) conducted a study in the Tadla plain aimed at mapping crop types through remote sensing techniques while evaluating various machine learning methods. The assessment of classifications yielded overall accuracies of 89.26%, 85.27%, and 57.17%, along with kappa indices of 0.85, 0.80, and 0.40 for Random Forest, Support Vector Machine, and Spectral Angle Mapper, respectively.

LULC change and prediction

LULC changes are fundamentally interconnected with geographical factors and development policies. An analysis of the transition occurring from 1993 to 2023 was conducted, utilizing spatiotemporal LULC data alongside physical and socioeconomic driving forces. This analysis facilitated the development of a transition probability matrix for each interval by utilizing the MOLUSCE plugin within QGIS software. Furthermore, Using the CA-ANN multilayer perceptron approach built into the MOLUSCE plugin, the LULC for 2033 was forecasted.

The obtained findings reveal a considerable transformation since 1993, characterized by a pronounced reduction in agricultural and forested areas. This decline is intricately associated with diminished precipitation (Kessabi et al., 2022), Agricultural practices in the region are significantly dependent on winter rainfall for irrigation purposes; thus, any reduction in precipitation, along with the rising frequency and severity of drought conditions (Hakam et al., 2023), directly impacts agricultural productivity. This decline not only disturbs crop yields but also amplifies wider environmental and socio-economic issues within the basin, heightening resource scarcity and increasing vulnerability of livelihoods. Furthermore, (El Hafyani et al., 2020) identified a comparable trend, marked by the growth of urban and agricultural areas at the expense of diminishing forest cover. (Salhi et al., 2024) reported an increase in dense forests alongside a reduction in agricultural lands within the N'fis Basin in recent decades.

These LULC transformations are influenced by climate change as well as human activities, which affect natural resources and the environment. The study emphasized the importance of a comprehensive management approach that harmonizes environmental preservation with socio-economic development in order to foster sustainability and resilience.

CONCLUSIONS

The study achieved its purpose by assessing that GB can demonstrate significant accuracy and reliability that greater than RF and SVM in classifying LULC. GB demonstrated greatest accuracy and Kappa (0.99) in the 2023 classifications and was the only method discerning temporal change in LULC classification. Furthermore, CA-ANN LULC prediction for 2033 was verified with Kappa index (77%) and demonstrates that this model can predict future changes with a degree of reliability.

A key scientific advancement from this research the introduction of spatial drivers (elevation and distance from roads) into predicted LULC, allowing for more nuanced understanding about how the terrain and access modify land transformation. This study indicates a trend of declines in agriculture and forest land along the emergence of bare soil and urban areas with consequences of the growing impacts of humans and potentially land abandonment, suggesting mounting pressure on ecosystems, biodiversity and food security.

This study contributes methodologically to the existing literature by providing a systematic comparison of different machine learning algorithms to monitor LULC in the long-term perspective, and by using simulation tools for elucidating land changes as related to observed trends. It also provides a reproducible method for other region in similar states of socio-environmental change.

It is exciting to think about some future work directions stemming from this research that include LULC modeling and climate and hydrological data in order to better evaluate the environmental implications of land change. Interdisciplinary approaches will be important in the future of land management for improving resilience in vulnerable landscapes and in sustainable development.

Acknowledgments

Thanks to the Moroccan Ministry of Higher Education, Scientific Research and Innovation and the OCP Foundation who funded this work through the APRD research program (GEANTech).

The first author thanks the CNRST through the “PhD-Associate Scholarship – PASS” Program. The authors express their appreciation to the representation of IRD in Morocco for its support.

REFERENCES

1. Agidew, Alem-meta Assefa, and Singh, K. N. (2017). The implications of land use and land cover changes for rural household food insecurity in the northeastern highlands of Ethiopia: The Case of the Teleyayen Sub-Watershed. *Agriculture & Food Security 6*(1): 56. https://doi.org/10.1186/s40066-017-0134-4
2. Ait Brahim, Y,, Seif-Ennasr, M., Malki, M,. N’da, B., Choukrallah, R. El Morjani, Z.E.A., Sifeddine, A., Abahous, H., and Bouchaou, L. (2017). Assessment of climate and land use changes: impacts on groundwater resources in the Souss-Massa River Basin. *The Souss-Massa River Basin, Morocco*, 121–142.
3. Ait El Haj, Fatiha, Latifa Ouadif, and Ahmed Akhssas. (2023). Monitoring land use and land cover change using remote sensing techniques and the precipitation-vegetation indexes in Morocco. *Ecological Engineering & Environmental Technology* 24(1): 272–286. https://doi.org/10.12912/27197050/154937
4. Akinyemi, F. O. (2021). Vegetation trends, drought severity and land use-land cover change during the growing season in semi-arid contexts. *Remote Sensing* 13(5): 836. https://doi.org/10.3390/rs13050836
5. Ayugi, B., Tan, G., Niu, R., Dong, Z., Ojara, M., Mumo, L., Babaousmail, H. and Ongoma, V. (2020). Evaluation of meteorological drought and flood scenarios over Kenya, East Africa. *Atmosphere* 11(3): 307. https://doi.org/10.3390/atmos11030307
6. Sardari, A., Reza, M., Bazrafshan, O., Panagopoulos,T., and Sardooi, E. R. (2019). Modeling the impact of climate change and land use change scenarios on soil erosion at the Minab Dam Watershed.” *Sustainability* 11(12): 3353. https://doi.org/10.3390/su11123353
7. Borrelli, P., Robinson, D. A., Panagos, P., Lugato, E., Yang, J. E., Alewell, C., Wuepper, D., Montanarella, L., and Ballabio, C. (2020). Land use and climate change impacts on global soil erosion by water (2015–2070). *Proceedings of the National Academy of Sciences* 117(36): 21994–22001. https://doi.org/10.1073/pnas.2001403117.

8. Bouchaou, L., Tagma, T., Boutaleb, S., Hssaisoune, M., and El Morjani, Z. E. A. (2011). Climate change and its impacts on groundwater resources in Morocco: The case of the Souss-Massa Basin. In *Climate Change Effects on Groundwater Resources: A Global Synthesis of Findings and Recommendations*, 129–151. https://doi.org/10.1201/b11611-13
9. Breiman, L. (2001). Random forests. *Machine Learning* 45: 5–32. https://doi.org/10.1023/A:1010933404324
10. El Hachimi, J., El Harti, A., Ouzemou, J. -E., Lhissou, R., Chakouri, M. and Jellouli, A. (2022). Assessment of the benefit of a single Sentinel-2 satellite image to small crop parcels mapping. *Geocarto International* 37 (25): 7398–7414. https://doi.org/10.1080/10106049.2021.1974955
11. El Hafyani, M., Essahlaoui, A., Van Rompaey, A., Mohajane, M., El Hmaidi, A., El Ouali, A., Moudden, F., and Serrhini, N.-E. (2020). Assessing regional scale water balances through remote sensing techniques: A case study of Boufakrane River Watershed, Meknes Region, Morocco. *Water* 12(2): 320. https://doi.org/10.3390/w12020320
12. Elaloui, A., El Khalki, E. M., Namous, M., Ziadi, K., Eloudi, H., Faouzi, E., Bou-Imajjane, L., Karroum, M., Tramblay, Y., Boudhar, A. and Chehbouni, A**.** (2022). Soil erosion under future climate change scenarios in a Semi-Arid Region. *Water* 15(1): 146. https://doi.org/10.3390/w15010146
13. Esmail, M., Masria, A. and Negm, A. (2016). Monitoring land use/land cover changes around Damietta promontory, Egypt, Using RS/GIS. *Procedia Engineering* 154: 936–942. https://doi.org/10.1016/j.proeng.2016.07.515
14. Fei, L., Shuwen, Z., Jiuchun, Y., Liping, C., Haijuan, Y., and Kun, B. (2018). Effects of land use change on ecosystem services value in West Jilin since the reform and opening of China. *Ecosystem Services* 31(June): 12–20. https://doi.org/10.1016/j.ecoser.2018.03.009
15. Hadri, A., El Mehdi Saidi, M. E. M. and Boudhar, A. (2021). Multiscale drought monitoring and comparison using remote sensing in a Mediterranean Arid Region: A case study from West-Central Morocco." *Arabian Journal of Geosciences* 14: 1–18. https://doi.org/10.1007/s12517-021-06493-w
16. Hakam, O., Baali, A., Azennoud, K., Lyazidi, A., and Bourchachen, M. (2023). Assessments of drought effects on plant production using satellite remote sensing technology, GIS and observed climate data in Northwest Morocco: Case of the Lower Sebou Basin. *International Journal of Plant Production*, 1–16. https://doi.org/10.1007/s42106-023-00237-7
17. Hakam, O., Ongoma, V., Beniaich, A., Meskour, B., El Kadi, M. A., Brouziyne, Y., Hssaisoune, M., Tairi, A., Labbaci, A., and Bouchaou, L. (2024). Assessment of the impact of climate change on argan tree in the mediterranean GIAHS Site, Morocco: Current and future distributions. *Modeling Earth Systems and Environment* 10(4): 5529–52.
18. Htitiou, A., Boudhar, A., Lebrini, Y., Hadria, R., Lionboui, H., Elmansouri, L., Tychon, B., and Benabdelouahab, T. (2019). The performance of random forest classification based on phenological metrics derived from Sentinel-2 and Landsat 8 to map crop cover in an irrigated Semi-Arid Region. *Remote Sensing in Earth Systems Sciences* 2(4): 208–24. https://doi.org/10.1007/s41976-019-00023-9
19. Idoumskine, I., Aydda, A., Ezaidi, A., Ramouch, K., and Haddou, M. A. (2024). Assessing impact of land use/land cover dynamic on urban climate change in a Semi-Arid Region–case study of Agadir City (Morocco). *Ecological Engineering* 4.
20. Jun, M.-J. (2021). A Comparison of a gradient boosting decision tree, random forests, and artificial neural networks to model urban land use changes: The case of the Seoul Metropolitan Area." *International Journal of Geographical Information Science* 35(11): 2149–67.
21. Kessabi, R., Hanchane, M., Krakauer, N. Y., Aboubi, I., El Kassioui, J., and El Khazzan, B. (2022). Annual, seasonal, and monthly rainfall trend analysis through non-parametric tests in the Sebou River Basin (SRB), Northern Morocco. *Climate* 10(11): 170.
22. Labbaci, A., and Bouchaou, L. (2022). Assessing land degradation and sensitivity to desertification using MEDALUS model and Google Earth Engine in a Semi-Arid Area in Southern Morocco: Case of Draa Watershed. *Frontiers in Science and Engineering* 11(January): Change and impact in southern Morocco: Evidence and understanding. https://doi.org/10.34874/IMIST.PRSM/FSEJOURNAL-V11I2.29049
23. Loukika, K. N., Keesara, V. R. and Sridhar, V. (2021). Analysis of land use and land cover using machine learning algorithms on Google Earth Engine for Munneru River Basin, India. *Sustainability* 13(24): 13758
24. Luo, N., Mao, D., Wen, B., Liu, X. (2020). Climate change affected vegetation dynamics in the Northern Xinjiang of China: Evaluation by SPEI and NDVI. *Land* 9, 90. https://doi.org/10.3390/land9030090
25. Martin, E. A., Feit, B., Requier, F., Friberg, H., Jonsson, M. (2019). Assessing the resilience of biodiversity-driven functions in agroecosystems under environmental change, in: *Advances in Ecological Research*. Elsevier, 59–123. https://doi.org/10.1016/bs.aecr.2019.02.003
26. IPCC (2013)., n.d. Climate change 2013: The physical science basis. In: Stocker TF, Qin D, Plattner G-K, Tignor M, Allen SK, Boschung J, Nauels A, Xia Y, Bex V, Midgley PM (eds) Contribution of working group I to the fifth assessment report of the intergovernmental panel on climate change.

Cambridge University Press, Cambridge.

27. McFeeters, S. K. (1996). The use of the normalized difference water index (NDWI) in the delineation of open water features. *International Journal of Remote Sensing* 17(7): 1425–1432. https://doi.org/10.1080/01431169608948714
28. McCarty, D. A., Kim, H. W., and Lee, H. K. (2020). Evaluation of light gradient boosted machine learning technique in large scale land use and land cover classification. *Environments* 7(10): 84.
29. Mohajane, M., Essahlaoui, A., Oudija, F., El Hafyani, M., El Hmaidi, A., El Ouali, A., Randazzo, G., and Teodoro, A. C. (2018). Land use/land cover (LULC) using Landsat data series (MSS, TM, ETM+ and OLI) in Azrou Forest, in the Central Middle Atlas of Morocco. *Environments* 5(12): 131. https://doi.org/10.3390/environments5120131
30. Muhammad, R., Zhang, W., Abbas, Z., Guo, F., and Gwiazdzinski, L. (2022). Spatiotemporal change analysis and prediction of future land use and land cover changes using QGIS MOLUSCE plugin and remote sensing big data: A case study of Linyi, China. *Land* 11(3): 419. https://doi.org/10.3390/land11030419
31. Muto, Y., Noda, K., Maruya, Y., Chibana, T., and Watanabe, S. (2022). Impact of climate and land-use changes on the water and sediment dynamics of the Tokoro River Basin, Japan. *Environmental Advances* 7: 100153.
32. Ongoma, V., Driouech, F., Brouziyne, Y., Chfadi, T., Terence Epule, T., Tanarhte, M., and Chehbouni, A. (2024). Morocco's climate change impacts, adaptation and mitigation – a Stocktake. *Regional Environmental Change* 24(1): 14.
33. Ouassanouan, Y., Fakir, Y., Simonneaux, V., Kharrou, M. H., Bouimouass, H., Najar, I., Benrhanem, M., Sguir, F., and Chehbouni, A. (2022). Multidecadal analysis of water resources and agricultural change in a mediterranean semiarid irrigated piedmont under water scarcity and human interaction. *Science of The Total Environment* 834: 155328.
34. Ouazar, D., Doukkali, M. R., Elyoussfi, L. and others. (2017). A mathematical model for assessment of socio-economic impact of climate change on agriculture activities: Cases of the East of Morocco (Africa). *Indian Journal of Science and Technology*.
35. Ouzemou, J.-E., El Harti, A., Lhissou, R., El Moujahid, A., Bouch, N., El Ouazzani, R., Bachaoui, E. M., and El Ghmari, A. (2018). Crop type mapping from pansharpened Landsat 8 NDVI Data: A case of a highly fragmented and intensive agricultural system. *Remote Sensing Applications: Society and Environment* 11: 94–103. https://doi.org/10.1016/j.rsase.2018.05.002
36. Pal, M., and Mather, P. M. (2005). Support vector machines for classification in remote sensing." *International Journal of Remote Sensing* 26(5): 1007–11.
37. Phuong, N. T., Khoa, N. P., Hung, L. T., Tung, P. G., Huy, L. Đ., Hai, N. Y., Ha, T. N., Ngu, N. H., and Duc, T. T. (2023). Evaluation and prediction of land use, and land cover changes using remote sensing and CA-ANN Model in Huong Hoa District, Quang Tri Province. *Hue University Journal of Science: Agriculture and Rural Development* 132(3C). https://doi.org/10.26459/hueunijard.v132i3C.7219
38. Saddik, A., Hssaisoune, M., Belaqziz, S., Labbaci, A., Tairi, A., Meskour, B., and Bouchaou, L. (2024). Assessing the health and yield of argan trees in Morocco's unique ecosystem: A multispectral and machine learning approach. *International Journal of Remote Sensing*, 1–29.
39. Salhi, W., Heddoun, O., Honnit, B., Saidi, M. N. and Kabbaj, A. (2024). Characterizing land use-land cover changes in N'fis Watershed, Western High Atlas, Morocco (1984–2022). *Applied Geomatics*, 1–15.
40. Talukdar, S., Singha, P., Mahato, S., Pal, S., Liou, Y.- A., and Rahman, A. (2020). Land-use land-cover classification by machine learning classifiers for satellite observations—a review. *Remote Sensing* 12(7): 1135.
41. Tavares, P. A., Beltrão, N., Guimarães, U. S., Teodoro, A., and Gonçalves, P. (2019). Urban ecosystem services quantification through remote sensing approach: a systematic review. *Environments* 6(5): 51. https://doi.org/10.3390/environments6050051
42. Vapnik, V. (1998). The Support Vector Method of Function Estimation. In *Nonlinear Modeling: Advanced Black-Box Techniques*, 55–85. Springer.
43. Zhao, Z., Islam, F., Waseem, L. A., Tariq, A., Nawaz, M., Ul Islam, I., Bibi, T., et al. (2024). Comparison of three machine learning algorithms using Google Earth engine for land use land cover classification. *Rangeland Ecology & Management* 92: 129–37. https://doi.org/10.1016/j.rama.2023.10.007